

Toward Practical Silicon Anodes: A Review of Composite Modification Strategies in Lithium-Ion Batteries

Shuai Wang

School of Materials Science and Engineering, Shandong Jianzhu University, Jinan, 250101, China

Abstract: In response to the increasing global demand for clean energy, lithium-ion batteries have been widely applied as one of the most efficient energy storage systems. Among various anode materials, silicon has attracted considerable attention due to its extremely high theoretical capacity. Nevertheless, its practical application is limited by severe volume expansion during the charge-discharge process, poor intrinsic electrical conductivity, and the instability of the solid electrolyte interphase. To overcome these issues, various compositing strategies have been developed. In these approaches, silicon is combined with conductive matrices, structural frameworks, or polymeric binders. These components help to improve mechanical robustness, enhance electrical conductivity, and stabilize the electrode interface. Therefore, a large number of studies have focused on the design and synthesis of silicon-based composite anode materials. This review summarizes recent developments in this field, with an emphasis on four major types of composites: Si-C, Si-metal, Si-metal oxide, and Si-polymer systems. The structural characteristics, functional roles, and electrochemical properties of each type are discussed in detail. In addition, this work also provides insights into future research directions and practical challenges of silicon-based anodes in advanced lithium-ion batteries.

Keywords: Lithium-Ion Batteries; Silicon Anodes; Composite Strategies

1. Introduction

With the continuous development of society and the growing global population, energy demand in various countries has increased significantly [1]. However, the excessive exploitation of conventional energy sources has not only exacerbated resource depletion but also caused severe environmental pollution and increased global greenhouse gas emissions [2,3]. Therefore, it is urgent to develop clean and renewable energy sources as alternatives to traditional fossil fuels [4]. Renewable energy sources such as solar, wind, nuclear, and tidal power are widely regarded as promising [5], but due to their unstable nature, it is necessary to employ efficient and high-capacity energy storage systems to store the generated energy. Among various energy storage technologies, secondary batteries have attracted extensive attention due to their high energy conversion efficiency and operational flexibility [6,7]. As a representative type of secondary battery, lithium-ion batteries (LIBs) have been widely applied in portable electronics, electric vehicles, and aerospace owing to their high energy density, low self-discharge rate, long cycle life, and minimal memory effect [8,9]. LIBs are mainly composed of four key components: cathode, anode, separator, and electrolyte. Among these components, the performance of the anode material plays a crucial role in the overall electrochemical performance of the battery. Currently, graphite remains the most mature and widely used anode material, with a theoretical capacity of only 372 mAh g^{-1} . To enhance the energy density of batteries, researchers are actively exploring novel anode materials with higher theoretical specific capacity, longer cycle life, better safety, and lower production costs [10]. Compared with the intercalation mechanism of graphite, lithium alloying reactions involving metals or metalloids such as Si, Pb, Ga, Sn, Ge, and Mg offer an effective approach to achieving higher capacities [11–14].

Silicon (Si), with its exceptionally high theoretical specific capacity ($\sim 4200 \text{ mAh g}^{-1}$), low working potential ($\sim 0.4 \text{ V vs. Li/Li}^+$), and abundant presence in the Earth's crust, is considered one of the most promising anode materials for LIBs, and has attracted extensive research interests [15]. However, despite these advantages, Si still faces significant challenges in practical applications. Firstly, as a semiconductor, Si has intrinsically low electrical conductivity, which limits its electronic transport efficiency within the electrode. More critically, during the lithiation/delithiation process, Si undergoes substantial volume changes of up to 300–400% [16,17]. This causes severe expansion and contraction, often leading to the loss

of contact between Si particles and the conductive network, resulting in rapid capacity fade and poor cycling stability [18]. Additionally, significant irreversible capacity loss is observed in the initial cycles [19]. The repeated fracture of the solid electrolyte interphase (SEI) due to volume changes exposes fresh Si surfaces to the electrolyte. This exposure causes continuous side reactions that further deteriorate capacity. As a result, irreversible capacity accumulation increases during cycling [20,21].

Therefore, effectively mitigating the volume expansion of Si during charge/discharge cycles is essential for enhancing its electrochemical performance and cycling stability. To address the volume change issue, a variety of strategies have been proposed, which can be classified into three categories: (1) Nanostructuring, where Si is designed at the nanoscale, such as nanoparticles, nanowires, nanotubes, thin films, and porous structures. They provide buffer space for expansion, reduce stress concentration, and mitigate particle pulverization, thereby improving cycling performance [21,22]; (2) Compositing Si with other materials through structural design and interfacial engineering to enhance the mechanical stability and electrical conductivity of electrodes [23–30]; (3) Using high-performance binders and electrolyte additives to maintain electrode structural integrity and SEI layer stability [31,32].

Among these strategies, compositing is considered one of the most promising approaches. This is due to its multiple advantages, including enhancing conductivity, alleviating volume expansion, and facilitating stable SEI formation. Additionally, compositing offers cost-effectiveness and design flexibility. Based on the type of composite components, Si-based composite materials can be categorized into the following types: (1) Si/C composites, including coated structures (core-shell, fibrous), embedded structures (e.g., graphene), and dispersed structures (e.g., pitch, organic polymers) [23–26]; (2) Si/metal composites, where Si is combined with conductive metals such as Ag, Cu, and Fe to enhance overall electrical conductivity and structural stability [27]; (3) Si/metal oxide composites, such as Al_2O_3 , which can serve as buffer layers to suppress volume expansion [28]; (4) Si/polymer composites can improve the overall performance of LIBs by enhancing conductivity, alleviating volume expansion, improving cycling stability, and increasing flexibility [29,30].

This review aims to systematically summarize recent studies on composite strategies of Si anodes. We will discuss various composite strategies in terms of design principles, electrochemical performance, and practical application potential. Figure 1 illustrates representative composite modification strategies for silicon-based anodes, categorized into four major types: Si-C composites, Si-metal composites, Si-metal oxide composites, and Si-polymer composites. Each part highlights typical nanostructures and material designs, such as core-shell architectures, porous frameworks, and hybrid interfaces that aim to mitigate the volume expansion of silicon and enhance its electrochemical performance. Detailed discussions of these strategies and their structural and functional advantages will be presented in the following sections.

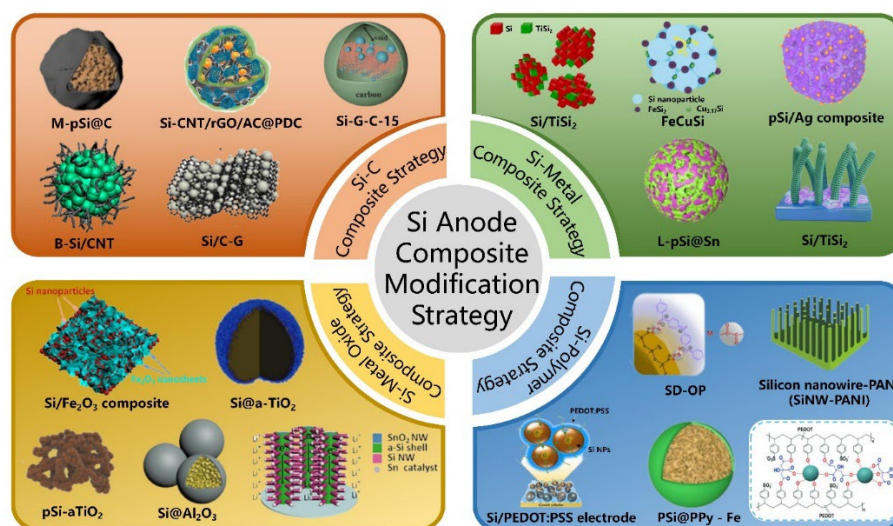


Figure 1: Schematic illustration of typical composite modification strategies for silicon-based anode materials.

2. Si-C Composite Modification Strategy

The composite of Si and C materials is an effective strategy for modifying silicon anodes, prepared through chemical methods based on silicon sources and various carbon materials, forming a composite structure with synergistic effects[33]. This composite material achieves a close integration of silicon and carbon at the micro or nanoscale, combining the excellent electronic conductivity and stability of carbon with the high specific capacity of silicon. This method not only increases the conductivity from 10^{-5} S/cm to 10^{-3} S/cm, but also effectively alleviates the impact of the inherent volume changes of silicon on cycling performance[34,35]. Si-C composites effectively address issues such as volume expansion, poor conductivity, and interface stability in lithium-ion battery silicon anodes. Typically, in Si-C composite materials for LIBs, carbon is introduced in the following forms: Graphite-like carbon (such as natural or artificial graphite) as a substrate or coating layer, providing conductivity and buffering volume changes[36,37]; Amorphous carbon (such as hard carbon, soft carbon) forms porous structures or serves as a coating layer by pyrolyzing organic materials, alleviating the volume expansion of silicon[38–40]; Nanocarbon materials (such as carbon nanotubes, graphene) build a three-dimensional conductive network with their high conductivity and mechanical flexibility, enhancing the structural stability of the material[41,42].

These composite strategies significantly enhance the cycling performance and rate capability of the silicon anode through synergistic effects. Core-shell structures or yolk-shell structures can be formed by coating silicon with carbon. These structures reduce direct contact between silicon and the electrolyte. As a result, they help suppress side reactions. They also prevent the repeated cracking and reconstruction of the SEI film. This reduces irreversible capacity loss and improves Coulombic efficiency[43,44]. The porous carbon structure provides fast lithium-ion transport channels, thereby overcoming the inherent conductivity deficiencies of silicon. It also dynamically adapts to the volume changes of silicon during charge and discharge through physical constraints and elastic deformation, which alleviates up to 300% volume expansion during lithiation/delithiation and suppresses particle fragmentation and electrode structure collapse [45,46]. Nanometer-scale carbon-silicon composite materials disperse local stress concentration, maintaining electrode integrity and reducing the detachment of active materials. The three-dimensional continuous conductive network constructed by highly conductive carbon nanomaterials (such as graphene, carbon nanotubes) not only reduces the contact resistance between silicon particles, facilitating electron transport, but also accelerates lithium-ion diffusion dynamics, significantly improving rate performance and extending cycle life[47–49].

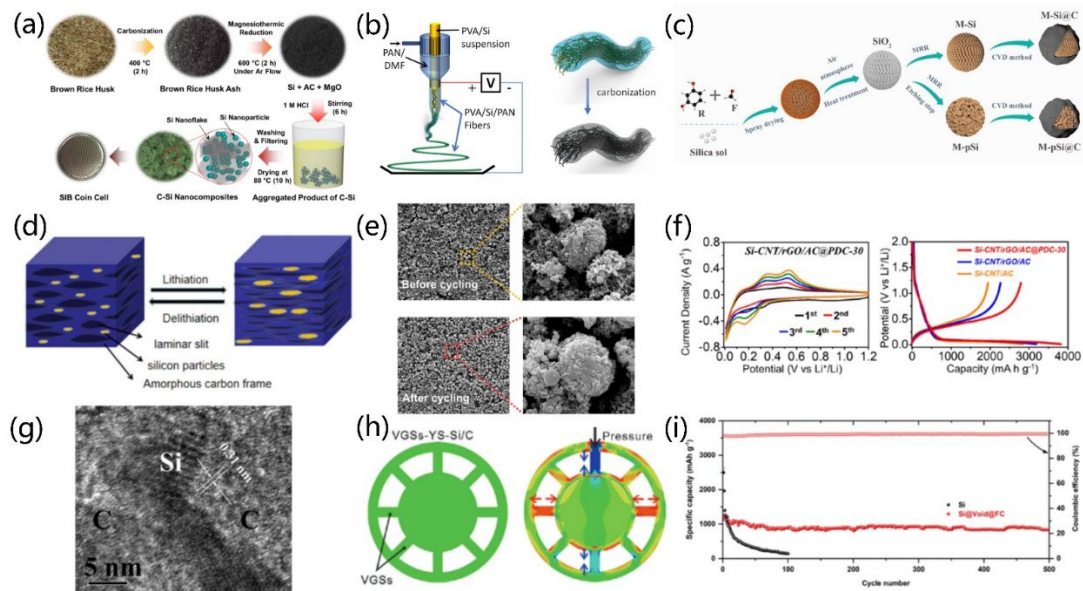


Figure 2: (a)-(i)

(a) One-Pot Synthesized Biomass C-Si Nanocomposites as an Anodic Material for High-Performance Sodium-Ion Battery[50]; (b) Nanofiber-in-Microfiber Carbon/Silicon Composite Anode with High Silicon Content for LIBs[25]; (c) Scalable Synthesis of Micrometer-Sized Porous Silicon/Carbon Composites for High-Stability Lithium-Ion Battery Anodes[51]; (d) Durable Flexible Dual-Layer and Free-Standing Silicon/Carbon Composite Anode for LIBs[52]; (e) An Innovative

Strategy for Constructing Multicore Yolk-Shell Si/C Anodes for LIBs[53]; (f) Pitch-Derived C Coated Three-Dimensional CNTs/Reduced Graphene Oxide Microsphere Encapsulating Si Nanoparticles as Anodes for LIBs[54]; (g) Scalable Synthesis of Interconnected Porous Silicon/Carbon Composites by the Rochow Reaction as High-Performance Anodes of LIBs[55]; (h) Hierarchical Yolk-Shell Silicon/Carbon Anode Materials Enhanced by Vertical Graphene Sheets for Commercial Lithium-Ion Battery Applications[56]; (i) Innovative Design of Silicon-Core Mesoporous Carbon Composite for High Performance Anode Material in Advanced LIBs[57].

In recent years, to mitigate critical challenges such as volume expansion and insufficient electrical conductivity of silicon-based anode materials during cycling, researchers have developed various structural designs of Si/C composites, resulting in significant performance improvements. For instance, a one-pot magnesiothermic reduction strategy using rice husk ash as the precursor was employed to construct a C-Si nanocomposite structure (Figure 2a) [50], where ultrasmall Si nanoparticles are densely encapsulated by highly conductive carbon nanosheets, delivering an impressive capacity retention of 98% after 100 cycles at 200 mA/g, indicating excellent cycling stability. By integrating coaxial electrospinning and carbonization, another type of nanofiber-microfiber composite was developed (Figure 2b) [25], in which the 3D conductive network and mesoporous buffer space effectively mitigate the volume variation and internal stress of silicon, resulting in approximately 90% capacity retention between the 50th and 250th cycles at a silicon content of 40%.

Furthermore, the M-pSi@C composite synthesized via spray drying and magnesiothermic reduction (Figure 2c) [51] features abundant porosity and interconnected channels, and exhibits outstanding rate capability and cycling stability under the synergistic effect of carbon coating, maintaining a capacity of 1702 mAh/g after 250 cycles at 1 A/g. In terms of flexible structures, microelectronic printing technology was utilized to fabricate a Si/C composite with a layered slit architecture (Figure 2d) [52], which can effectively accommodate the volume expansion of silicon during lithiation, preventing electrode structure degradation, with a capacity retention of 81.8% after 100 cycles and excellent rate performance at 1 A/g.

In addition, a yolk-shell Si/C composite constructed via spray drying and in-situ growth of MOF-derived carbon shells (Figure 2e) [53] eliminates the need for a sacrificial template and forms a hollow cavity and stable SEI film, significantly enhancing structural integrity and conductivity during cycling, achieving a reversible capacity of 1054.5 mAh/g after 100 cycles. To further enhance electron transport efficiency, Si/C composite microspheres were proposed, comprising a 3D conductive network of 1D CNTs, 2D rGO, and amorphous carbon, further coated with pitch-derived carbon (PDC) (Figure 2f) [54]. This structure delivered initial charge/discharge capacities of 3814/2791 mAh/g with a Coulombic efficiency of 73.2%, while also facilitating electrochemical reaction kinetics.

Regarding interfacial structure optimization, a porous Si/C composite fabricated by tuning Rochow reaction conditions (Figure 2g) [55] forms interfacial voids between Si and carbon coating that accommodate volume changes during lithiation/delithiation, thereby enhancing cycling stability. On the other hand, the VGSS-YS-Si/C composite synthesized by thermal chemical vapor deposition (Figure 2h) [56], supported by finite element simulations, shows that its graphene sheets effectively disperse compressive stress, enhancing the mechanical integrity of the carbon shell and achieving a high capacity retention of 80.1% after 1000 cycles at 1 C. Meanwhile, the hollow core-shell structured Si@Void@FC composite (Figure 2i) [57], with a carbon shell serving as both buffer and barrier layer, accommodates silicon expansion and reduces electrolyte contact, achieving a capacity of 838 mAh/g and 74% retention after 500 cycles.

These Si/C composites, through systematic structural, interfacial, and conductive network designs, not only alleviate the volume expansion issue but also significantly enhance electrical conductivity and SEI film stability. Diverse structural strategies—including core-shell, yolk-shell, 3D conductive networks, and porous flexible scaffolds—exhibit synergistic enhancements in cycle life and rate capability, offering essential technological pathways and theoretical foundations for developing high-energy-density, long-life, and scalable silicon-based anodes.

3. Si-Metal Composite Modification Strategy

The combination of silicon with metals (M) represents a significant strategy for anode modification. This composite is typically synthesized via physical methods or chemical approaches, resulting in the formation of binary or ternary metal silicides with the general formula M_xSi_y . Compared to pure silicon, these metal silicides offer enhanced structural support, thereby improving the structural stability of the electrode material. They can also synergize with silicon through reversible electrochemical reactions,

effectively mitigating issues such as volumetric expansion and poor electrical conductivity[58,59].

In LIBs anode materials, metals can be classified based on whether they form compounds with lithium atoms, and are categorized as active metals (Ma) and inactive metals (Mi). Active metals include elements such as Mg[60], Ge[61,62], Ca[63], Ag[64], Sn[65,66], and Al[67–69], whereas Ni[70,71], Fe[72–74], Cu[75,76], and Ti[51,77–79] are considered inactive metals[80]. In Si-Ma composite systems, both silicon and active metals can participate in electrochemical reactions with lithium ions, thereby significantly enhancing the specific capacity of the battery. Because the formation potentials of different lithiated phases vary, volumetric expansion does not occur simultaneously, enabling a stepwise release of mechanical stress. One component often acts as a buffering matrix for the other, forming Li-Si alloys and a secondary lithiated product during charge-discharge cycles. This secondary phase typically exists in the form of pure metal or metal compounds, which helps to mitigate the volumetric expansion during lithiation[60–69,81–83]. In contrast, in Si-Mi composite systems, the inactive metal does not react with lithium itself, but merely serves as a structural support framework. It provides buffering and conductive pathways for silicon without directly participating in the lithiation process[70–80,84].

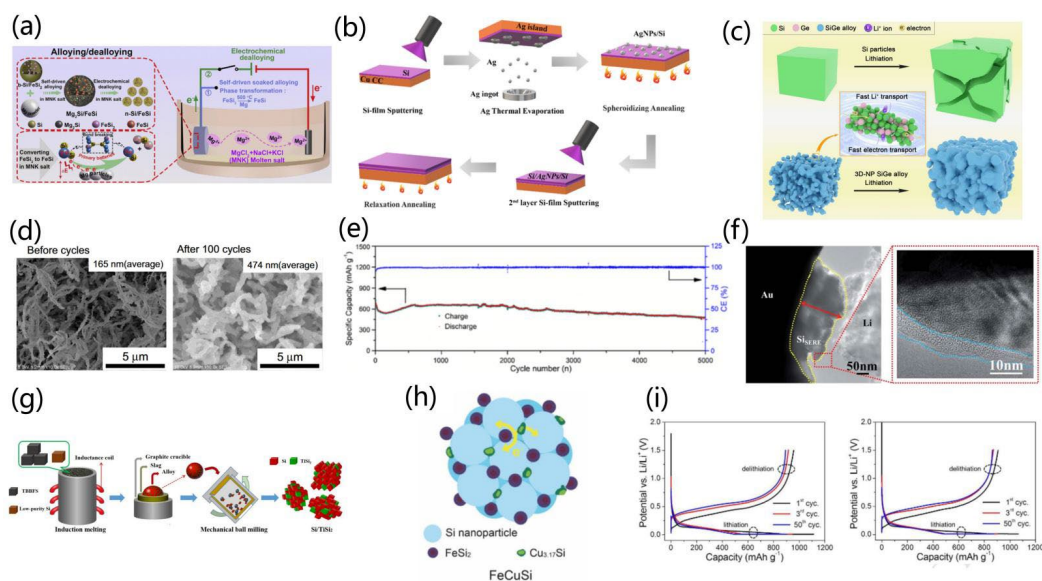


Figure 3: (a)-(i)

(a) Electrochemically Converting Micro-Sized Industrial Si/FeSi₂ to Nano Si/FeSi for the High-Performance Lithium-Ion Battery Anode[85]; (b) Scalable Interlayer Nanostructure Design for High-Rate (10C) Submicron Silicon-Film Electrode by Incorporating Silver Nanoparticles[86]; (c) Morphology- and Porosity-Tunable Synthesis of 3D-Nanoporous SiGe Alloy as High-Performance Lithium-Ion Battery Anode[87]; (d) Single-Step Fabrication of Fibrous Si/Sn Composite Nanowire Anodes by High-Pressure He Plasma Sputtering for High-Capacity Li-Ion Batteries[88]; (e) Ultrathin Silicon Nanolayer Implanted NiSi/Ni Nanoparticles as Superlong-Cycle Lithium-Ion Anode Material[89]; (f) Crystalline Cu-Silicide Stabilizes the Performance of a High Capacity Si-Based Li-Ion Battery Anode[90]; (g) Constructing Cycle-Stable Si/TiSi₂ Composites as Anode Materials for LIBs Through Direct Utilization of Low-Purity Si and Ti-Bearing Blast Furnace Slag[91]; (h) Micron-Sized Fe–Cu–Si Ternary Composite Anodes for High Energy Li-Ion Batteries[92]; (i) High Capacity Retention Si/Silicide Nanocomposite Anode Materials Fabricated by High-Energy Mechanical Milling for Lithium-Ion Rechargeable Batteries[93].

In recent years, researchers have designed a series of innovative silicon/metal composite materials through various synthesis methods such as radio frequency magnetron sputtering, dealloying, high-energy ball milling, and electrochemical dealloying, which have demonstrated excellent performance in structural optimization, volume expansion mitigation, and conductivity enhancement.

Ma et al. used a self-driven alloying-electrochemical dealloying method to prepare nano-Si/FeSi (n-Si/FeSi). As shown in Figure 3(a) [85], bulk ferrosilicon alloy (b-Si/FeSi₂) is first mixed with Mg powder and placed in an MNK molten salt (MgCl₂ + NaCl + KCl) to form a galvanic cell at 500°C, which allows Mg to extract some Si from FeSi₂ to form FeSi/Mg₂Si alloy. The resulting alloy is then electrochemically treated in the molten salt system to selectively remove Mg from the alloy, ultimately obtaining n-Si/FeSi. Similarly, in a study where Si/AgNPs/Si multilayer thin film electrodes were prepared by RF magnetron

sputtering and thermal evaporation methods (Figure 3b) [86], the introduction of silver nanoparticles effectively suppressed the volume expansion and crack formation of silicon, significantly enhancing the material's capacity, reaching 1250 mAh/g at a 10C rate, three times that of pure silicon material, and showing good capacity retention. The success of this design indicates that appropriate nanoparticle filling can significantly improve the electrochemical performance of silicon-based anode materials.

Similarly, the three-dimensional nanoporous SiGe alloy prepared by dealloying (Figure 3c) [87] also demonstrates its excellent electrochemical properties. The excellent electronic conductivity and fast lithium-ion migration properties of germanium have significantly improved the material's rate performance and cycling stability. Its three-dimensional nanostructure not only effectively accommodates volume changes but also accelerates Li^+ transport, further enhancing the material's electrochemical performance. Additionally, the Si/Sn nanowire composite material (Figure 3d) [88] prepared by helium plasma sputtering showed no significant pulverization even after 100 cycles, despite an increase in the diameter of the silicon nanowires. This indicates that the design of one-dimensional nanowires can effectively alleviate physical strain and improve cycling stability, thus maintaining the material's good performance. The results of this study further demonstrate the importance of structural design in enhancing battery stability.

Another study prepared Ni_xSi nanoparticles with a nickel core (Figure 3e) [89] through high-energy ball milling and annealing processes. The gradient distribution structure of this material not only enhanced the electrode's conductivity but also provided mechanical support during the lithiation/delithiation process, ensuring that the material maintained a high capacity after 5000 cycles. This indicates that the introduction of the nickel core plays a key role in maintaining the structural stability of the composite material. The nanoporous $\text{Si}/\text{Cu}_{0.83}\text{Si}_{0.17}/\text{Cu}$ composite material (Figure 3f) [90], prepared using a ternary Cu-Si-Al alloy as the precursor and a sulfur-assisted dealloying process, showed almost no visible degradation during lithiation and exhibited excellent volume expansion mitigation. This innovative structural design effectively improved the material's stability and electrochemical performance. Similarly, the Si/TiSi_2 composite material (Figure 3g) [91], prepared using a combination of induction melting and mechanical ball milling, exhibited excellent electrochemical performance at high current densities, particularly demonstrating its potential in resource recycling during the use of low-purity Si and metallurgical waste recovery.

Furthermore, the Fe-Cu-Si ternary composite material (Figure 3h) [92], with its unique porous dual-phase structure, shows significant advantages in mitigating silicon volume expansion and enhancing conductivity. Through spray drying and thermal treatment, this material exhibited high initial Coulombic efficiency and specific capacity during cycling, proving its great potential for practical applications. Finally, the $\text{Si}_{80}\text{Fe}_{16}\text{Cr}_4$ composite material (Figure 3i) [93] synthesized by high-energy mechanical milling showed excellent stability during long-term cycling, further confirming the broad application prospects of silicon-based composite materials in battery technology.

4. Si-Metal Oxide Composite Modification Strategy

Silicon/metal oxide (Si/MO) composites are typically synthesized by combining metal oxides with silicon via methods such as sol-gel processing or combustion reactions. Unlike silicon/metal composites, Si/MO composites often exhibit a core-shell structure, where the metal oxide generally serves as a robust coating material, similar in concept to silicon/carbon core-shell structures [94,95]. This architecture effectively mitigates the volume expansion of silicon during lithiation/delithiation, enhances the stability of the SEI, and reduces undesirable side reactions between silicon and the electrolyte [96–99].

Commonly used metal oxides include TiO_2 [100,101], Al_2O_3 [28], ZnO [102,103], SnO_2 [104], CuO [105], Fe_2O_3 [106], Nb_2O_5 [107], Co_3O_4 [108], $\text{W}_{18}\text{O}_{49}$ [109], and MoO_3 [110]. These oxides are mostly derived from transition metals, though some are from main-group elements. Metal oxides are typically coated onto the surface of silicon particles. The outer oxide layer, with its insulating nature and high dielectric constant, can function as an artificial SEI layer. This coating structure effectively suppresses the volumetric changes of silicon during lithium insertion/extraction. Moreover, metal oxide coatings exhibit excellent corrosion resistance, which helps prevent electrolyte-induced degradation of silicon particles. They also inhibit excessive SEI formation and stabilize interfacial reactions, thereby enhancing the structural integrity and cycling stability of the Si/MO composite anode materials [59,111–113].

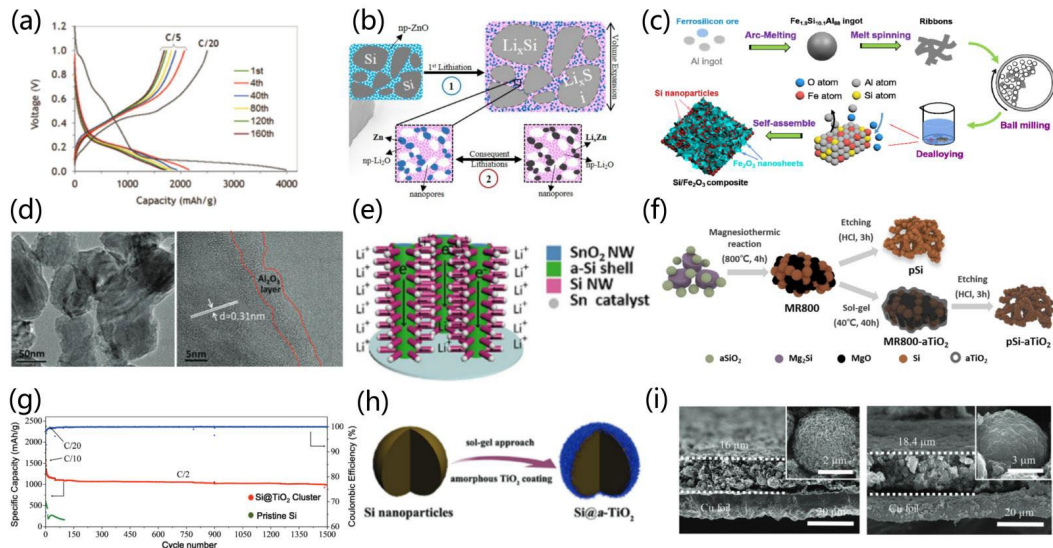


Figure 4: (a)-(i)

(a) Interfacial Stabilizing Effect of ZnO on Si Anodes for Lithium-Ion Battery[103]; (b) Conversion Reaction of Nanoporous ZnO for Stable Electrochemical Cycling of Binderless Si Microparticle Composite Anode[102]; (c) Porous Si/Fe₂O₃ Dual Network Anode for Lithium-Ion Battery Application[114]; (d) An Al₂O₃ Coating Layer on Mesoporous Si Nanospheres for Stable SEI and High-Rate Capacity for LIBs[115]; (e) Hierarchical Nano-Branched c-Si/SnO₂ Nanowires for High Areal Capacity and Stable Lithium-Ion Battery[116]; (f) Novel Synthesis of Porous Si-TiO₂ Composite as a High-Capacity Anode Material for Li Secondary Batteries[117]; (g) Self-Healing SEI Enables Full-Cell Cycling of a Silicon-Majority Anode with a Coulombic Efficiency Exceeding 99.9%[118]; (h) Amorphous TiO₂ Shells: A Vital Elastic Buffering Layer on Silicon Nanoparticles for High-Performance and Safe Lithium Storage[119]; (i) Silicon-Based Self-Assemblies for High Volumetric Capacity Li-Ion Batteries via Effective Stress Management[120].

Zinc oxide (ZnO) coatings play an important role in enhancing the mechanical stability and electrochemical performance of silicon-based anodes. By depositing ZnO protective coatings on the surface of silicon nanoparticles, researchers found that the voltage curve showed no significant changes after 160 charge-discharge cycles, demonstrating good cycling stability. Even after 260 cycles, the reversible capacity could still maintain 1500 mAh·g⁻¹ (Figure 4a) [103]. ZnO was coated on silicon microparticle electrodes using a simple and scalable combustion reaction method. The electrode material generated by this method converts ZnO into a Li₂O matrix containing conductive Zn nanoparticles during charge and discharge processes, greatly accelerating electron transfer and preventing electrode pulverization. Even after 210 cycles at a C/5 rate, the electrode capacity still remained at 1500 mAh·g⁻¹ (Figure 4b) [102].

Another study prepared a porous Si/Fe₂O₃ composite material using melt-spinning and ball milling methods. The mesoporous structure of this material effectively accommodates the volume changes during the lithiation/delithiation process, enhancing the diffusion rate of lithium ions and demonstrating excellent electrochemical performance. At a current density of 200 mA·g⁻¹, after 100 cycles, the material's reversible capacity still remained at 697.2 mAh·g⁻¹ (Figure 4c) [114]. The Si@Al₂O₃ composite material prepared using aluminum nanospheres with a natural Al₂O₃ layer as a template exhibited excellent volume change mitigation and lithium ion transport efficiency. After 120 cycles, the material's specific capacity reached 1750.2 mAh·g⁻¹, and after 500 cycles, it still maintained a high capacity of 1001.7 mAh·g⁻¹ (Figure 4d left) [115]. A hierarchical Si/SnO₂ nanowire structure was also designed as an anode material for lithium-ion batteries. By using SnO₂ nanowires as a scaffold and Si nanowires as a high-capacity lithium ion storage medium, this structure not only provides excellent electrical contact but also facilitates rapid charge and discharge processes. After 100 cycles, the material still maintained a capacity of 1200 mAh·g⁻¹ and exhibited good mechanical integrity, without the need for conductive agents or binders (Figure 4e) [116].

Additionally, amorphous TiO₂, as a coating material, played a protective role on the porous silicon nanostructure. By controlling the size and ratio of the raw materials, a porous silicon structure with a

TiO₂ coating was successfully synthesized, demonstrating an initial specific capacity of up to 3487 mAh·g⁻¹ in electrochemical tests, and maintaining a capacity of 1965 mAh·g⁻¹ after 100 cycles (Figure 4f) [117]. A self-healing artificial solid electrolyte interface (aSEI) structure was designed, in which the TiO₂ shell effectively encapsulated silicon particles, enabling them to accommodate volume expansion. In the initial cycle, the electrode's Coulombic efficiency was 65.8%, and after 1500 cycles, the specific capacity remained at 990 mAh·g⁻¹ (Figure 4g) [118]. Finally, a sol-gel method was used to coat amorphous TiO₂ on the surface of silicon particles, demonstrating good lithium ion conductivity and safety. The material reached a specific capacity of 1720 mAh·g⁻¹ after 200 cycles at a current density of 420 mA·g⁻¹, and still maintained a high capacity at higher rates (Figure 4h)[119]. The Si@TiO₂@C composite material, designed through multi-scale simulations, combines a TiO₂ layer and carbon filling, effectively suppressing electrode cracking caused by volume changes while ensuring mechanical stability. After 1000 cycles, the material still maintained a capacity of 842.6 mAh·g⁻¹, demonstrating excellent long-term stability (Figure 4i) [120].

These studies suggest that the incorporation of metal oxides (such as ZnO, TiO₂) with silicon-based materials can significantly improve the electrochemical performance, mechanical stability, and cycling life of silicon anode materials, providing valuable experience and theoretical support for the design and application of future silicon-based anode materials.

5. Si-Polymer Composite Modification Strategy

The combination of Si and polymers involves tightly integrating silicon materials with polymers via methods such as in situ polymerization or sol-gel processing. This approach aims to construct a composite system that offers both high specific capacity and excellent flexibility and conductivity, thereby significantly enhancing the overall performance of silicon electrodes in lithium-ion batteries [121–123]. This composite strategy effectively mitigates several critical issues associated with silicon anodes during cycling, including volume expansion, instability of the SEI, and poor electronic conductivity [124–126]. Commonly studied conductive polymers include polyaniline (PANI) [127–129], polypyrrole (PPy) [130,131], poly(3,4-ethylenedioxythiophene) (PEDOT) [132,133], and its derivative PEDOT:PSS [134,135], which exhibit good electrical conductivity as well as excellent mechanical flexibility and film-forming properties [136–138]. Conductive polymers possess desirable electrochemical properties, tunable molecular structures, and outstanding mechanical compatibility; during charge-discharge cycles, their functional groups can interact with the oxidized surface of silicon via strong hydrogen bonding, forming a protective layer akin to an elastic coating. This structural design helps buffer the volume changes induced by lithium insertion, reducing the risk of electrode pulverization and mechanical failure, thereby maintaining electrode integrity and extending cycle life.

Furthermore, conductive polymers form a three-dimensional electron transport network among silicon particles, offering continuous pathways for electron conduction and significantly enhancing the electronic conductivity of the electrode material, thereby improving the rate performance of the battery. Additionally, some polymers can function as binders, strengthening the adhesion between active materials and the current collector, thus effectively preventing delamination of electrode materials during repeated charge-discharge cycles [127–138].

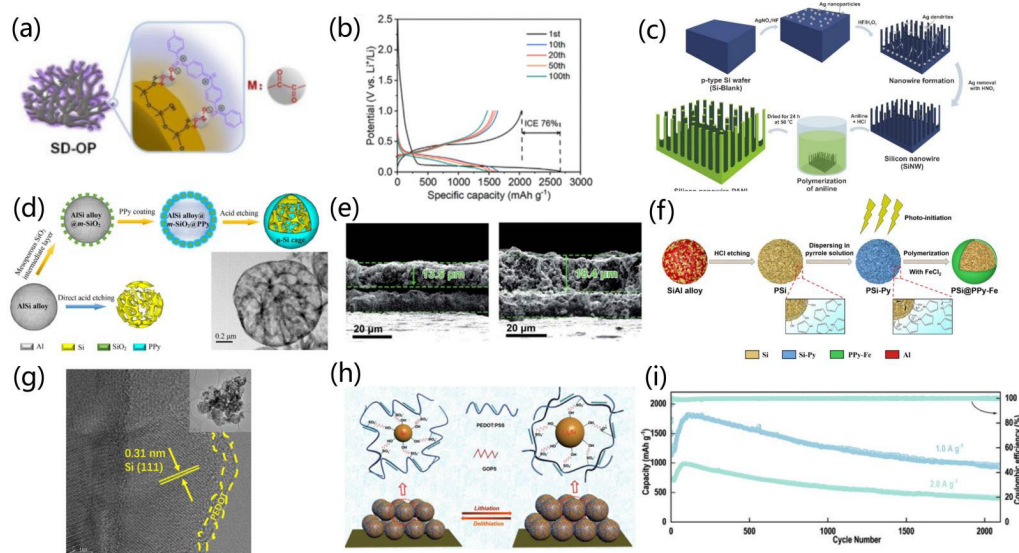


Figure 5: (a)-(i)

(a) Carbon-Free Silicon/Polyaniline Hybrid Anodes with 3D Conductive Structures for Superior LIBs[139]; (b) Integrating SEI into Layered Conductive Polymer Coatings for Ultrastable Silicon Anodes[140]; (c) A Free-Standing Polyaniline/Silicon Nanowire Forest as the Anode for LIBs[141]; (d) Largely Improved Battery Performance Using a Microsized Silicon Skeleton Caged by Polypyrrole as Anode[142]; (e) Interpenetrating Gels as Conducting/Adhering Matrices Enabling High-Performance Silicon Anodes[143]; (f) Photo-Initiated in Situ Synthesis of Polypyrrole Fe-Coated Porous Silicon Microspheres for High-Performance Lithium-Ion Battery Anodes[144]; (g) Studies on the Preparation and Electrochemical Performance of PSi@Poly(3, 4-Ethylenedioxythiophene) Composites as Anode Materials for LIBs[145]; (h) Chemical Coupled PEDOT:PSS/Si Electrode: Suppressed Electrolyte Consumption Enables Long-Term Stability[146]; (i) Enhanced Silicon Anodes with Robust SEI Formation Enabled by Functional Conductive Binder[147].

In recent studies, typical conductive polymers have included PANI, PPy, and PEDOT. Through methods such as in-situ polymerization, chemical cross-linking, and interface engineering, these polymers can form flexible conductive networks on silicon surfaces, stabilize the SEI layer, and significantly enhance both cycling and rate performance.

As a representative conjugated conductive polymer, PANI possesses highly tunable redox states and strong interfacial adhesion, making it suitable for in-situ construction of both buffering and conductive layers. In one study, a star-shaped PANI-based conductive binder was designed, where the three-dimensional conjugated network enhanced structural flexibility and electronic conductivity, significantly improving the cycling stability of the Si anode, with a capacity of 1776 mAh g^{-1} retained after 100 cycles [128]. To further enhance the coating effect, another study employed an oxalic acid-assisted strategy to direct the polymerization of aniline on the surface of coral-like nano-silicon (Figure 5a) [139]. This approach avoids the use of conventional conductive additives by forming a dense and uniform conductive network, delivering a capacity of 610 mAh g^{-1} after 1000 cycles at 1C with an initial coulombic efficiency of 85.9%, demonstrating excellent interfacial stability. Meanwhile, constructing structurally directed layered coatings has also been proven to be an effective way to improve performance. For instance, Pan et al. developed a layered conductive PANI (LCP) coating (Figure 5b) [140], using TMSPA cross-linkers and tungstic acid to induce in-plane polymer alignment, which guided uniform SEI formation and delivered excellent rate capability and cycle life under high areal capacity ($\sim 3 \text{ mAh cm}^{-2}$). In another study, researchers applied a metal-assisted chemical etching (MACE) method to fabricate vertically aligned silicon nanowire forests, followed by in-situ polymerization of PANI (Figure 5c) [141], enabling high surface area electron pathways while maintaining structural integrity, with an areal capacity of 2.0 mAh cm^{-2} retained after 346 cycles.

Compared to PANI, PPy offers higher intrinsic conductivity and chemical stability, making it widely used for constructing flexible conductive networks or coatings. For example, one study reported the use of a TEOS sol-gel strategy to pre-form a mesoporous SiO_2 interlayer, followed by surface polymerization of PPy to create a hollow “ μ -Si cage” structure (Figure 5d) [142], which provides buffering space while ensuring both electron and ion pathways. This material exhibited a capacity retention of 83.8% after 400

cycles at 0.2C. In addition, PPy can also form interpenetrating network structures in conjunction with polymer binders. By simultaneously initiating oxidative polymerization of PPy and crosslinking of PVA, a uniformly distributed gel network was formed among Si particles (Figure 5e) [143], enhancing mechanical toughness and mitigating particle detachment. This composite achieved a high capacity of 1834 mAh g⁻¹ with stable cycling at 0.5A g⁻¹. Notably, light-induced in-situ polymerization offers a novel route for constructing conductive polymer coatings. By exploiting the photo-generated hole effect of Si, an in-situ growth of PPy-Fe coatings was induced, forming yolk-shell PSi@PPy-Fe microspheres (Figure 5f) [144], which exhibited excellent rate performance and maintained a capacity of 1853.7 mAh g⁻¹ after 200 cycles.

PEDOT exhibits excellent film-forming ability and environmental stability, and is commonly employed to enhance the overall electronic conductivity of electrodes. Using in-situ polymerization, a dense and uniform PEDOT coating can be formed on porous silicon (PSi) surfaces (Figure 5g) [145], effectively reducing irreversible capacity loss caused by SEI layer formation. At 0.5A g⁻¹, the fabricated electrode retained 70.3% of its capacity after 200 cycles. To further strengthen interfacial bonding, GOPS silane crosslinkers were introduced to bind PEDOT:PSS to the Si surface, forming a three-dimensional elastic conductive network (Figure 5h) [146]. This method significantly improved the structural integrity and cycling stability of the electrode, with a capacity of 1957.6 mAh g⁻¹ retained after 200 cycles. Building on this, modulation of PEDOT:PSS conformations can impart self-healing capabilities to the material. Chen et al. introduced a dual-modification system using citric acid (CA) and isopropanol (IPA) to construct a self-healing three-dimensional conductive network (Figure 5i) [147], thereby greatly enhancing the strain-relief ability of the electrode structure and achieving ~1000 mAh g⁻¹ capacity with 89% retention after 2000 cycles at 1A g⁻¹.

6. Summary and Outlook

Silicon-based anode materials are widely regarded as highly promising candidates for LIBs due to their high theoretical specific capacity and low lithiation potential. However, silicon undergoes significant volume expansion, resulting in electrode structural degradation and repeated rupture/reformation of the SEI. This review systematically summarizes recent key advances in this field, particularly focusing on composite strategies involving carbon materials, metals, metal oxides, and polymers, with representative electrochemical performance parameters listed in Table 1. As shown in Table 1, Si-C composites exhibit significant advantages in cycling stability and rate performance; Si-metal composites demonstrate high initial coulombic efficiency and excellent cycle life; Si-metal oxide composites typically deliver high specific capacities; and Si-conductive polymer composites show favorable interfacial adaptability and flexible encapsulation effects.

Table 1: Summary of the Performance of Selected Composite-Modified Silicon-Based Anode Materials for LIBs

Classification	Materials	Capacity (mAh·g ⁻¹ @ A·g ⁻¹)	Cycling stability (cycles@ A·g ⁻¹)	Initial Coulomb efficiency (%)	Ref
Si-C Composite Modification Strategy	Si-C	941.1@0.1,421.6@1.0	769.8 (100@0.1)	79	[52]
	Si-C	2418@0.1,1257.4@2	734.8(400@1)	71.4	[53]
	Si-CNT/ rGO/AC@PDC	3814@0.1,617@2	947 (350@1)	73.2	[54]
	pSi@void@NFC	3012.2@0.1,447.6 @12	866(1000@6)	86.9	[24]
	Si@Void@FC	1138@0.5,787@2	838(500@0.5)	71.	[57]
	C@Si-GP(121)	1052.3@0.1,394.57@2	715.0(800@0.2)	87.24	[148]
	Si@C@CNS	1110@1,283@10	682(500@1)	70	[35]
Si-Metal Composite Modification Strategy	Si@C	3095.0@0.1,1382.4@5	934.5(300@3)	89.8	[149]
	Si-Ge	1670@0.1C,613@10C	1180(400@0.2C)	74.7	[81]
	Si/TiSi ₂	1184.1@0.1,422.3@1.6	530(200@0.8)	95.6	[91]
	Cu ₃ Si/Si	2530.7@0.2,776.1@1.6	1675.4(100@0.2)	88.94	[76]
	n-Si/FeSi@C	1676@0.2,1199@2	846.8(1500@2)	99.5	[85]
	pSi/Ag	3677@0.1,1778@2	1930(50@1)	89.09	[86]
	Si-Ti	1532@0.1,500@8	1017(300@2)	94.8	[77]
	Si ₁₂ Ge ₈	1558@1,577@8	1158(150@1)	75.6	[87]
	Si/Sn	977@0.01 C	580(135@0.1C)	>95	[88]
	Si@NixSi/Ni	706.1 @0.5,472@2	521.5(5000@0.5)	81.5	[89]

	Si/TiSi ₂	1936.1 @0.2	1133.8(200@0.2)	83.99	[78]
Si-Metal Oxide Composite Modification Strategy	pSi-a-TiO ₂	3800 @0.1	1965(100@0.5)	90.1	[117]
	Si@a-TiO ₂	3061@0.42,128@8.4	~1720(200@0.42)	~86.1	[119]
	Si/Fe ₂ O ₃	3167.7@0.2,512.2@5	697.2 (100@0.2)	70.5	[114]
	np-ZnO/SiMP	3900@0.05C	1500(200@0.2C)	117	[102]
	Si@TiO ₂ @C	~823@6	842.6(1000@2)	80.9	[120]
	Si@Al ₂ O ₃	3371.3 @0.5,416.2@20	1001.7(500@2)	73	[115]
	Si/ZnO	2600@0.05C	1500(260@0.5C)	63	[103]
	Si@TiO ₂	2374@0.05C,1070@0.5C	990(1500@0.5C)	65.8	[118]
	HN-Si@aTiO ₂	2804.6@1,749.2@4	524.6(500@5)	78.47	[100]
	Si@SnO ₂	3239@0.2,506@5	1000(200@2)	84.1	[112]
	Si@TiO ₂	2399.9@0.2,815.0@3	1174.4(100@1)	73.3	[111]
	μ-Si cage	~1980@0.2C,1161@1C	868(1500@2C)	78.2	[142]
Si-Polymer Composite Modification Strategy	PSi@PPy-Fe	2447.1@0.1,1558.4@4	557.7(1000@8)	77.7	[144]
	Si@PPy	3692.3@0.1,1546.3@1	1047.0(500@1)	83.3	[131]
	SiNPs-TMSPA-LCP	942@5	>1000(300@1)	76	[140]
	Si@PEDOT,	2461.3 @0.1,1168@2	1266.1(100@1)	61.6	[132]
	PSi@PEDOT	2553.5@0.5,313@4	878(200@0.5)	68.0	[145]
	Si@PP@CA	2440@0.2	979(2000@1)	72.1	[147]
	Si@PTh	2398.4,451.8@8	1130.5(1000@1)	65.3	[138]

Through compositing with different materials, silicon's volume change during charge/discharge can be effectively mitigated, while electron/ion transport and the number of active sites are enhanced, ultimately enabling higher energy density, faster charge/discharge rates, and longer cycle life for LIBs. These advances have greatly expanded the research framework of silicon-based anodes and provided new design concepts and material construction strategies for commercial application. Moreover, although there remain considerable controversies and unresolved issues regarding the microscopic mechanisms of silicon's volume effect and the evolution of the SEI during cycling, several studies have provided in-depth clarification of key processes. In addition to improving capacity and cycle performance through structural and material design, effectively suppressing the inhomogeneous growth of the SEI and mechanical fracture of silicon particles remains a major challenge.

To further enhance the overall performance of silicon anodes, continued exploration of novel multicomponent composite strategies and interface engineering approaches is needed. Such efforts will facilitate the development of more stable structural systems and improve the overall reversibility and structural integrity of the electrode. By integrating in situ characterization techniques (such as SEM, XRD, Raman, and XPS) to investigate the evolution of electrode structure, electrode/electrolyte interfacial reactions, and charge storage mechanisms, and combining these with theoretical simulations to explore electron and ion transport in electrode materials, it is expected that these approaches will offer essential theoretical guidance and practical direction for developing high-performance, low-cost, and scalable silicon-based anode materials. Undoubtedly, this represents a highly promising direction for future research.

Acknowledgement

Investigation, writing-original draft preparation and visualization: S.W.. The author have read and agreed to the published the manuscript.

References

- [1] D' Silva TC, Isha A, Chandra R, Vijay VK, Subbarao PMV, Kumar R, et al. Enhancing methane production in anaerobic digestion through hydrogen assisted pathways – a state-of-the-art review. *Renew Sustain Energy Rev* 2021;151:111536. <https://doi.org/10.1016/j.rser.2021.111536>.
- [2] Kumar A, Yau Y-Y, Ogita S, Scheibe R, editors. *Climate change, photosynthesis and advanced biofuels: the role of biotechnology in the production of value-added plant bio-products*. Singapore: Springer Singapore; 2020. <https://doi.org/10.1007/978-981-15-5228-1>.
- [3] Olabi AG, Wilberforce T, Abdelkareem MA. Fuel cell application in the automotive industry and future perspective. *Energy* 2021;214:118955. <https://doi.org/10.1016/j.energy.2020.118955>.
- [4] Li W, Zhang J, Wang W. Progress on nano- to atom-size dual-metal-site catalysts (DMSC) for

- enhanced dry reforming of methane with carbon dioxide. *Coord Chem Rev* 2024;503:215638. <https://doi.org/10.1016/j.ccr.2023.215638>.
- [5] Khan N, Dilshad S, Khalid R, Kalair AR, Abas N. Review of energy storage and transportation of energy. *Energy Storage* 2019;1:e49. <https://doi.org/10.1002/est2.49>.
- [6] Solangi KH, Islam MR, Saidur R, Rahim NA, Fayaz H. A review on global solar energy policy. *Renew Sustain Energy Rev* 2011;15:2149–63. <https://doi.org/10.1016/j.rser.2011.01.007>.
- [7] Luo X, Wang J, Dooner M, Clarke J. Overview of current development in electrical energy storage technologies and the application potential in power system operation. *Appl Energy* 2015;137:511–36. <https://doi.org/10.1016/j.apenergy.2014.09.081>.
- [8] Huang X, Yang J, Mao S, Chang J, Hallac PB, Fell CR, et al. Controllable synthesis of hollow si anode for long-cycle-life lithium-ion batteries. *Adv Mater* 2014;26:4326–32. <https://doi.org/10.1002/adma.201400578>.
- [9] Li M, Lu J, Chen Z, Amine K. 30 years of lithium-ion batteries. *Adv Mater* 2018;30:1800561. <https://doi.org/10.1002/adma.201800561>.
- [10] Wu F, Maier J, Yu Y. Guidelines and trends for next-generation rechargeable lithium and lithium-ion batteries. *Chem Soc Rev* 2020;49:1569–614. <https://doi.org/10.1039/C7CS00863E>.
- [11] Yi T-F, Zhu Y-R, Tao W, Luo S, Xie Y, Li X-F. Recent advances in the research of $\text{MLi}_2\text{Ti}_6\text{O}_{14}$ ($M = 2\text{Na}, \text{sr}, \text{ba}, \text{pb}$) anode materials for li-ion batteries. *J Power Sources* 2018;399:26–41. <https://doi.org/10.1016/j.jpowsour.2018.07.086>.
- [12] Li Q, Xu C, Yang L, Pei K, Zhao Y, Liu X, et al. Pb/C composite with spherical pb nanoparticles encapsulated in carbon microspheres as a high-performance anode for lithium-ion batteries. *ACS Appl Energy Mater* 2020;3:7416–26. <https://doi.org/10.1021/acsaem.0c00812>.
- [13] Liu X, Wu X-Y, Chang B, Wang K-X. Recent progress on germanium-based anodes for lithium ion batteries: efficient lithiation strategies and mechanisms. *Energy Storage Mater* 2020;30:146–69. <https://doi.org/10.1016/j.ensm.2020.05.010>.
- [14] Xin F, Whittingham MS. Challenges and development of tin-based anode with high volumetric capacity for li-ion batteries. *Electrochem Energy Rev* 2020;3:643–55. <https://doi.org/10.1007/s41918-020-00082-3>.
- [15] Wen CJ, Huggins RA. Chemical diffusion in intermediate phases in the lithium-silicon system. *J Solid State Chem* 1981;37:271–8. [https://doi.org/10.1016/0022-4596\(81\)90487-4](https://doi.org/10.1016/0022-4596(81)90487-4).
- [16] Choi J, Kim G, Kim SY. Silicon graphite composite anode degradation: effects of silicon ratio, current density, and temperature. *Energy Technol* 2023;11:2201444. <https://doi.org/10.1002/ente.202201444>.
- [17] Sun L, Liu Y, Shao R, Wu J, Jiang R, Jin Z. Recent progress and future perspective on practical silicon anode-based lithium ion batteries. *Energy Storage Mater* 2022;46:482–502. <https://doi.org/10.1016/j.ensm.2022.01.042>.
- [18] Li P, Zhao G, Zheng X, Xu X, Yao C, Sun W, et al. Recent progress on silicon-based anode materials for practical lithium-ion battery applications. *Energy Storage Mater* 2018;15:422–46. <https://doi.org/10.1016/j.ensm.2018.07.014>.
- [19] Jiang J, Zhang H, Zhu J, Li L, Liu Y, Meng T, et al. Putting nanoarmors on yolk-shell si@C nanoparticles: A reliable engineering way to build better si-based anodes for li-ion batteries. *ACS Appl Mater Interfaces* 2018;10:24157–63. <https://doi.org/10.1021/acsaami.8b07737>.
- [20] Etacheri V, Marom R, Elazari R, Salitra G, Aurbach D. Challenges in the development of advanced li-ion batteries: A review. *Energy Environ Sci* 2011;4:3243. <https://doi.org/10.1039/c1ee01598b>.
- [21] Chan CK, Peng H, Liu G, McIlwrath K, Zhang XF, Huggins RA, et al. High-performance lithium battery anodes using silicon nanowires. *Nat Nanotechnol* 2008;3:31–5. <https://doi.org/10.1038/nnano.2007.411>.
- [22] Salah M, Murphy P, Hall C, Francis C, Kerr R, Fabretto M. Pure silicon thin-film anodes for lithium-ion batteries: a review. *J Power Sources* 2019;414:48–67. <https://doi.org/10.1016/j.jpowsour.2018.12.068>.
- [23] Li X, Wu M, Feng T, Xu Z, Qin J, Chen C, et al. Graphene enhanced silicon/carbon composite as anode for high performance lithium-ion batteries. *RSC Adv* 2017;7:48286–93. <https://doi.org/10.1039/C7RA09818A>.
- [24] Zhou P, Xiao P, Pang L, Jiang Z, Hao M, Li Y, et al. High-performance yolk-shell structured silicon-carbon composite anode preparation via one-step gas-phase deposition and etching technique. *Adv Funct Mater* 2025;35:2406579. <https://doi.org/10.1002/adfm.202406579>.
- [25] Pei Y, Wang Y, Chang A-Y, Liao Y, Zhang S, Wen X, et al. Nanofiber-in-microfiber carbon/silicon composite anode with high silicon content for lithium-ion batteries. *Carbon* 2023;203:436–44. <https://doi.org/10.1016/j.carbon.2022.11.100>.
- [26] Xue X, Liu X, Lou B, Yang Y, Shi N, Wen F, et al. The mitigation of pitch-derived carbon with different

- structures on the volume expansion of silicon in si/C composite anode. *J Energy Chem* 2023;84:292–302. <https://doi.org/10.1016/j.jechem.2023.04.004>.
- [27] Song H, Wang HX, Lin Z, Jiang X, Yu L, Xu J, et al. Highly connected silicon–copper alloy mixture nanotubes as high-rate and durable anode materials for lithium-ion batteries. *Adv Funct Mater* 2016;26:524–31. <https://doi.org/10.1002/adfm.201504014>.
- [28] Xu K, Zhang Z, Su W, Wei Z, Zhong G, Wang C, et al. Alumina coated nano silicon synthesized by aluminothermic reduction as anodes for lithium ion batteries. *Funct Mater Lett* 2017;10:1650073. <https://doi.org/10.1142/S1793604716500739>.
- [29] Balqis F, Eldona C, Laksono BT, Aini Q, Hamid FH, Wasisto HS, et al. Conductive polymer frameworks in silicon anodes for advanced lithium-ion batteries. *ACS Appl Polym Mater* 2023;5:4933–52. <https://doi.org/10.1021/acsapm.3c00531>.
- [30] Zhang B, Liu D, Xie H, Wang D, Hu C, Dai L. In-situ construction of chemically bonded conductive polymeric network for high-performance silicon microparticle anodes in lithium-ion batteries. *J Power Sources* 2022;539:231591. <https://doi.org/10.1016/j.jpowsour.2022.231591>.
- [31] Yu L, Liu J, He S, Huang C, Gan L, Gong Z, et al. A novel high-performance 3D polymer binder for silicon anode in lithium-ion batteries. *J Phys Chem Solids* 2019;135:109113. <https://doi.org/10.1016/j.jpcs.2019.109113>.
- [32] Ren X, Huang T, Yu A. Carboxymethylated tamarind polysaccharide gum as a green binder for silicon-based lithium-ion battery anodes. *Electrochem Commun* 2022;136:107241. <https://doi.org/10.1016/j.elecom.2022.107241>.
- [33] Zuo P, Yin G, Ma Y. Electrochemical stability of silicon/carbon composite anode for lithium ion batteries. *Electrochimica Acta* 2007;52:4878–83. <https://doi.org/10.1016/j.electacta.2006.12.061>.
- [34] Shen X, Tian Z, Fan R, Shao L, Zhang D, Cao G, et al. Research progress on silicon/carbon composite anode materials for lithium-ion battery. *J Energy Chem* 2018;27:1067–90. <https://doi.org/10.1016/j.jechem.2017.12.012>.
- [35] Xu Z, Du J, Feng C, He J, Li T, Jia H, et al. Constructing a buffer macroporous architecture on silicon/carbon anode for high-performance lithium-ion battery. *J Mater Sci Mater Electron* 2024;35:531. <https://doi.org/10.1007/s10854-024-12237-9>.
- [36] Wang A, Liu F, Wang Z, Liu X. Self-assembly of silicon/carbon hybrids and natural graphite as anode materials for lithium-ion batteries. *RSC Adv* 2016;6:104995–5002. <https://doi.org/10.1039/C6RA20131H>.
- [37] Ko M, Chae S, Ma J, Kim N, Lee H-W, Cui Y, et al. Scalable synthesis of silicon-nanolayer-embedded graphite for high-energy lithium-ion batteries. *Nat Energy* 2016;1:16113. <https://doi.org/10.1038/nenergy.2016.113>.
- [38] Lv D, Yang L, Song R, Yuan H, Luan J, Liu J, et al. A hierarchical porous hard carbon@si@soft carbon material for advanced lithium-ion batteries. *J Colloid Interface Sci* 2025;678:336–42. <https://doi.org/10.1016/j.jcis.2024.09.009>.
- [39] Li S, Qin X, Zhang H, Wu J, He Y-B, Li B, et al. Silicon/carbon composite microspheres with hierarchical core–shell structure as anode for lithium ion batteries. *Electrochem Commun* 2014;49:98–102. <https://doi.org/10.1016/j.elecom.2014.10.013>.
- [40] Wang D, Kong L, Zhang F, Liu A, Huang H, Liu Y, et al. Porous carbon-coated silicon composites for high performance lithium-ion batterie anode. *Appl Surf Sci* 2024;661:160076. <https://doi.org/10.1016/j.apsusc.2024.160076>.
- [41] Chen C, Zheng R, Ye L, Yue F, Cheng J, Wang J, et al. In situ synthesis of vertical graphene on porous si microparticle composite for high-performance anode material. *Electrochimica Acta* 2024;497:144617. <https://doi.org/10.1016/j.electacta.2024.144617>.
- [42] Zou X, Li M, Li H, Cao G, Jiang Q, Duan R, et al. Three-dimensional CNTs boosting the conductive confinement structure of silicon/carbon anodes in lithium-ion batteries. *Chem Eng J* 2024;498:155573. <https://doi.org/10.1016/j.cej.2024.155573>.
- [43] Xue L, Xu G, Li Y, Li S, Fu K, Shi Q, et al. Carbon-coated si nanoparticles dispersed in carbon nanotube networks as anode material for lithium-ion batteries. *ACS Appl Mater Interfaces* 2013;5:21–5. <https://doi.org/10.1021/am3027597>.
- [44] Zhou R, Fan R, Tian Z, Zhou Y, Guo H, Kou L, et al. Preparation and characterization of core–shell structure si/C composite with multiple carbon phases as anode materials for lithium ion batteries. *J Alloys Compd* 2016;658:91–7. <https://doi.org/10.1016/j.jallcom.2015.10.217>.
- [45] Shi L, Wang W, Wang A, Yuan K, Jin Z, Yang Y. Si nanoparticles adhering to a nitrogen-rich porous carbon framework and its application as a lithium-ion battery anode material. *J Mater Chem A* 2015;3:18190–7. <https://doi.org/10.1039/C5TA03974F>.
- [46] Shi H, Zhang W, Wang D, Wang J, Wang C, Xiong Z, et al. Facile preparation of silicon/carbon composite with porous architecture for advanced lithium-ion battery anode. *J Electroanal Chem*

- 2023;937:117427. <https://doi.org/10.1016/j.jelechem.2023.117427>.
- [47] Ni C, Xia C, Liu W, Xu W, Shan Z, Lei X, et al. Effect of graphene on the performance of silicon-carbon composite anode materials for lithium-ion batteries. *Materials* 2024;17:754. <https://doi.org/10.3390/ma17030754>.
- [48] Kang HE, Ko J, Song SG, Yoon YS. Recent progress in utilizing carbon nanotubes and graphene to relieve volume expansion and increase electrical conductivity of si-based composite anodes for lithium-ion batteries. *Carbon* 2024;219:118800. <https://doi.org/10.1016/j.carbon.2024.118800>.
- [49] Yang S, Li B, Yang Z, Song Y, Wang G, Yu F. Silicon-doped multilayer graphene as anode material for secondary batteries. *Appl Surf Sci* 2025;681:161483. <https://doi.org/10.1016/j.apsusc.2024.161483>.
- [50] Sekar S, Aqueel Ahmed AT, Kim DY, Lee S. One-pot synthesized biomass C-si nanocomposites as an anodic material for high-performance sodium-ion battery. *Nanomaterials* 2020;10:1728. <https://doi.org/10.3390/nano10091728>.
- [51] Su H, Li X, Liu C, Shang Y, Liu H. Scalable synthesis of micrometer-sized porous silicon/carbon composites for high-stability lithium-ion battery anodes. *Chem Eng J* 2023;451:138394. <https://doi.org/10.1016/j.cej.2022.138394>.
- [52] Zhang M, Li J, Sun C, Wang Z, Li Y, Zhang D. Durable flexible dual-layer and free-standing silicon/carbon composite anode for lithium-ion batteries. *J Alloys Compd* 2023;932:167687. <https://doi.org/10.1016/j.jallcom.2022.167687>.
- [53] Qiao Y, Hu Y, Qian Z, Qu M, Liu Z. An innovative strategy for constructing multicore yolk-shell si/C anodes for lithium-ion batteries. *J Colloid Interface Sci* 2025;684:678–89. <https://doi.org/10.1016/j.jcis.2025.01.078>.
- [54] Lee JS, Jo BS, Park J-S, Cho JS. Pitch-derived C coated three-dimensional CNTs/reduced graphene oxide microsphere encapsulating si nanoparticles as anodes for lithium-ion batteries. *Electrochimica Acta* 2025;512:145440. <https://doi.org/10.1016/j.electacta.2024.145440>.
- [55] Zhang Z, Wang Y, Ren W, Tan Q, Chen Y, Li H, et al. Scalable synthesis of interconnected porous silicon/carbon composites by the rochow reaction as high-performance anodes of lithium ion batteries. *Angew Chem Int Ed* 2014;53:5165–9. <https://doi.org/10.1002/anie.201310412>.
- [56] Yu P, Li Z, Zhang D, Xiong Q, Yu J, Zhi C. Hierarchical yolk-shell silicon/carbon anode materials enhanced by vertical graphene sheets for commercial lithium-ion battery applications. *Adv Funct Mater* 2025;35:2413081. <https://doi.org/10.1002/adfm.202413081>.
- [57] Yu Y, Zhang Q, Teng N, Liu Y. Innovative design of silicon-core mesoporous carbon composite for high performance anode material in advanced lithium-ion batteries. *J Alloys Compd* 2024;989:174423. <https://doi.org/10.1016/j.jallcom.2024.174423>.
- [58] Nuhu BA, Bamisile O, Adun H, Abu UO, Cai D. Effects of transition metals for silicon-based lithium-ion battery anodes: a comparative study in electrochemical applications. *J Alloys Compd* 2023;933:167737. <https://doi.org/10.1016/j.jallcom.2022.167737>.
- [59] Zhang X, Wang L, Zheng T, Lam K. Synthesis, electrochemistry, and thermal stability of high-energy ball-milled silicon-based alloy anodes in lithium-ion batteries**. *Batter Supercaps* 2023;6:e202200495. <https://doi.org/10.1002/batt.202200495>.
- [60] Nazer NS, Denys RV, Andersen HF, Arnberg L, Yartys VA. Nanostructured magnesium silicide Mg₂Si and its electrochemical performance as an anode of a lithium ion battery. *J Alloys Compd* 2017;718:478–91. <https://doi.org/10.1016/j.jallcom.2017.05.163>.
- [61] Adegoke TE, Abdul Ahad S, Bangert U, Geaney H, Ryan KM. Solution processable si/ge heterostructure NWs enabling anode mass reduction for practical full-cell li-ion batteries. *Nanoscale Adv* 2023;5:6514–23. <https://doi.org/10.1039/D3NA00648D>.
- [62] Stokes K, Boonen W, Geaney H, Kennedy T, Borsa D, Ryan KM. Tunable core-shell nanowire active material for high capacity li-ion battery anodes comprised of PECVD deposited aSi on directly grown ge nanowires. *ACS Appl Mater Interfaces* 2019;11:19372–80. <https://doi.org/10.1021/acsami.9b03931>.
- [63] Oh S-Y, Imagawa H, Itahara H. Si-based nanocomposites derived from layered CaSi₂: influence of synthesis conditions on the composition and anode performance in li ion batteries. *J Mater Chem A* 2014;2:12501–6. <https://doi.org/10.1039/C4TA01318B>.
- [64] Xi F, Zhang Z, Wan X, Li S, Ma W, Chen X, et al. High-performance porous silicon/nanosilver anodes from industrial low-grade silicon for lithium-ion batteries n.d.
- [65] Wang J-T, Lu S-G, Wang Y, Huang B, Yang J-Y, Tan A. Improvement of cycle behavior of si/sn anode composite supported by stable si-O-C skeleton. *Rare Met* 2022;41:1647–51. <https://doi.org/10.1007/s12598-014-0377-1>.
- [66] Yin J, Xu Z, Xiao Z, Shao H, Wang J. Photo/electrochemical synthesis of si@sn microsphere composites with excellent electrochemical lithium storage. *J Alloys Compd* 2022;900:163438. <https://doi.org/10.1016/j.jallcom.2021.163438>.
- [67] Galashev AY, Vorob'ev AS. First principle modeling of a silicene-aluminum composite anode for

- lithium ion batteries. *J Phys Chem Solids* 2023;181:111491. <https://doi.org/10.1016/j.jpccs.2023.111491>.
- [68] Kawaura H, Suzuki R, Nagasako N, Oh-ishi K. Scalable synthesis of porous silicon electrodes for lithium-ion batteries via acid etching of atomized al-si alloy powders. *J Power Sources* 2024;610:234739. <https://doi.org/10.1016/j.jpowsour.2024.234739>.
- [69] Suh S, Choi H, Eom K, Kim H-J. Enhancing the electrochemical properties of a si anode by introducing cobalt metal as a conductive buffer for lithium-ion batteries. *J Alloys Compd* 2020;827:154102. <https://doi.org/10.1016/j.jallcom.2020.154102>.
- [70] Ohta R, Gerile N, Kaga M, Kambara M. Composite si-ni nanoparticles produced by plasma spraying physical vapor deposition for negative electrode in li-ion batteries. *Nanotechnology* 2021;32:265703. <https://doi.org/10.1088/1361-6528/abef2b>.
- [71] Jia H, Stock C, Kloepsch R, He X, Badillo JP, Fromm O, et al. Facile synthesis and lithium storage properties of a porous NiSi_2 /si/carbon composite anode material for lithium-ion batteries. *ACS Appl Mater Interfaces* 2015;7:1508–15. <https://doi.org/10.1021/am506486w>.
- [72] Avila Cardenas A, Beaudhuin M, Nguyen LHB, Herlin-Boime N, Haon C, Monconduit L. An optimized electrically conductive si-fe matrix to boost the performance of si electrodes in li-ion batteries. *Energy Storage Mater* 2025;75:104086. <https://doi.org/10.1016/j.ensm.2025.104086>.
- [73] Ruttart M, Sizios V, Winter M, Placke T. Mechanochemical synthesis of fe-si-based anode materials for high-energy lithium ion full-cells. *ACS Appl Energy Mater* 2020;3:743–58. <https://doi.org/10.1021/acsaem.9b01926>.
- [74] Kumar P, Berhaut CL, Zapata Dominguez D, De Vito E, Tardif S, Pouget S, et al. Nano-architected composite anode enabling long-term cycling stability for high-capacity lithium-ion batteries. *Small* 2020;16:1906812. <https://doi.org/10.1002/sml.201906812>.
- [75] Stokes K, Geaney H, Sheehan M, Borsa D, Ryan KM. Copper silicide nanowires as hosts for amorphous si deposition as a route to produce high capacity lithium-ion battery anodes. *Nano Lett* 2019;19:8829–35. <https://doi.org/10.1021/acs.nanolett.9b03664>.
- [76] Jiang S, Cheng J, Nayaka GP, Dong P, Zhang Y, Xing Y, et al. Efficient electrochemical synthesis of Cu_3Si /si hybrids as negative electrode material for lithium-ion battery. *J Alloys Compd* 2024;998:174996. <https://doi.org/10.1016/j.jallcom.2024.174996>.
- [77] Lee P, Tahmasebi MH, Ran S, Boles ST, Yu DYW. Leveraging titanium to enable silicon anodes in lithium-ion batteries. *Small* 2018;14:1802051. <https://doi.org/10.1002/sml.201802051>.
- [78] Wang L, Niu Y, Liu H, Xi F, Yu J, Li S, et al. Preparation of si/ TiSi_2 as high-performance anode material for lithium-ion batteries by molten salt electrolysis. *J Alloys Compd* 2024;1008:176597. <https://doi.org/10.1016/j.jallcom.2024.176597>.
- [79] Xu J, Jin M, Shi X, Li Q, Gan C, Yao W. Preparation of TiSi_2 powders with enhanced lithium-ion storage via chemical oven self-propagating high-temperature synthesis. *Nanomaterials* 2021;11:2279. <https://doi.org/10.3390/nano11092279>.
- [80] Domi Y, Usui H, Takaishi R, Sakaguchi H. Lithiation and delithiation reactions of binary silicide electrodes in an ionic liquid electrolyte as novel anodes for lithium-ion batteries. *ChemElectroChem* 2019;6:581–9. <https://doi.org/10.1002/celc.201801088>.
- [81] Stokes K, Flynn G, Geaney H, Bree G, Ryan KM. Axial si-ge heterostructure nanowires as lithium-ion battery anodes. *Nano Lett* 2018;18:5569–75. <https://doi.org/10.1021/acs.nanolett.8b01988>.
- [82] Kim H, Son Y, Park C, Lee M-J, Hong M, Kim J, et al. Germanium silicon alloy anode material capable of tunable overpotential by nanoscale si segregation. *Nano Lett* 2015;15:4135–42. <https://doi.org/10.1021/acs.nanolett.5b01257>.
- [83] Stokes K, Geaney H, Flynn G, Sheehan M, Kennedy T, Ryan KM. Direct synthesis of alloyed $\text{si}_{1-x}\text{ge}_x$ nanowires for performance-tunable lithium ion battery anodes. *ACS Nano* 2017;11:10088–96. <https://doi.org/10.1021/acsnano.7b04523>.
- [84] Liu Y, Zhong Y, Zeng Z, Zhang P, Zhang H, Zhang Z, et al. Scalable synthesis of a porous micro si/si-ti alloy anode for lithium-ion battery from recovery of titanium-blast furnace slag. *ACS Appl Mater Interfaces* 2023;15:54539–49. <https://doi.org/10.1021/acsaami.3c13643>.
- [85] Ma Q, Zhao Y, Hu Z, Qu J, Zhao Z, Xie H, et al. Electrochemically converting micro-sized industrial si/ FeSi_2 to nano si/ FeSi for the high-performance lithium-ion battery anode. *Mater Today Energy* 2021;21:100817. <https://doi.org/10.1016/j.mtener.2021.100817>.
- [86] Chen Y-X, Liao H-C, Cheng Y-W, Huang J-H, Liu C-P. Scalable interlayer nanostructure design for high-rate (10C) submicron silicon-film electrode by incorporating silver nanoparticles. *ACS Appl Mater Interfaces* 2023;15:18845–56. <https://doi.org/10.1021/acsaami.2c23279>.
- [87] Yang Y, Liu S, Bian X, Feng J, An Y, Yuan C. Morphology- and porosity-tunable synthesis of 3D nanoporous SiGe alloy as a high-performance lithium-ion battery anode. *ACS Nano* 2018;12:2900–8. <https://doi.org/10.1021/acsnano.8b00426>.
- [88] Uchida G, Masumoto K, Sakakibara M, Ikebe Y, Ono S, Koga K, et al. Single-step fabrication of

fibrous si/sn composite nanowire anodes by high-pressure he plasma sputtering for high-capacity li-ion batteries. *Sci Rep* 2023;13:14280. <https://doi.org/10.1038/s41598-023-41452-3>.

[89] Tamirat AG, Lui Y, Dong X, Wang C, Wang Y, Xia Y. Ultrathin silicon nanolayer implanted ni_x si/ni nanoparticles as superlong-cycle lithium-ion anode material. *Small Struct* 2021;2:2000126. <https://doi.org/10.1002/ssstr.202000126>.

[90] Ma W, Liu X, Wang X, Wang Z, Zhang R, Yuan Z, et al. Crystalline cu-silicide stabilizes the performance of a high capacity si-based li-ion battery anode. *J Mater Chem A* 2016;4:19140–6. <https://doi.org/10.1039/C6TA08740J>.

[91] Zhang Y, Chen M, Chen Z, Wang Y, Li S, Duan P, et al. Constructing cycle-stable si/TiSi₂ composites as anode materials for lithium ion batteries through direct utilization of low-purity si and ti-bearing blast furnace slag. *J Alloys Compd* 2021;876:160125. <https://doi.org/10.1016/j.jallcom.2021.160125>.

[92] Chae S, Ko M, Park S, Kim N, Ma J, Cho J. Micron-sized fe–cu–si ternary composite anodes for high energy li-ion batteries. *Energy Environ Sci* 2016;9:1251–7. <https://doi.org/10.1039/C6EE00023A>.

[93] Han HK, Loka C, Yang YM, Kim JH, Moon SW, Cho JS, et al. High capacity retention si/silicide nanocomposite anode materials fabricated by high-energy mechanical milling for lithium-ion rechargeable batteries. *J Power Sources* 2015;281:293–300. <https://doi.org/10.1016/j.jpowsour.2015.01.122>.

[94] Wang F, Chen G, Zhang N, Liu X, Ma R. Engineering of carbon and other protective coating layers for stabilizing silicon anode materials. *Carbon Energy* 2019;1:219–45. <https://doi.org/10.1002/cey2.24>.

[95] Xu K, Liu X, Guan K, Yu Y, Lei W, Zhang S, et al. Research progress on coating structure of silicon anode materials for lithium-ion batteries. *ChemSusChem* 2021;14:5135–60. <https://doi.org/10.1002/cssc.202101837>.

[96] John J. Conformal coating of TiO₂ shell on silicon nanoparticles for improved electrochemical performance in li-ion battery applications n.d.

[97] Kowalski D, Mallet J, Thomas S, Nemaga AW, Michel J, Guery C, et al. Electrochemical synthesis of 1D core-shell si/TiO₂ nanotubes for lithium ion batteries. *J Power Sources* 2017;361:243–8. <https://doi.org/10.1016/j.jpowsour.2017.07.003>.

[98] Zhang N, Liu Y, Yang J, Zhang S, He S. Preparation and characterization of nanosized multi-sphere si-TiO₂ based composites for lithium storage. *Electrochimica Acta* 2016;212:657–61. <https://doi.org/10.1016/j.electacta.2016.07.044>.

[99] Sun C, Pan J, Fu X, Ma D, Cui L, Yao W, et al. Homogeneous encapsulation of si/SnO₂ nanospheres in tunable carbon electrospinning nanofibers for high-performance lithium-ion battery. *J Energy Storage* 2024;88:111576. <https://doi.org/10.1016/j.est.2024.111576>.

[100] Jiao X-W, Tian Y-H, Zhang X-J. Hollow si nanospheres with amorphous TiO₂ layer used as anode for high-performance li-ion battery. *Appl Surf Sci* 2021;566:150682. <https://doi.org/10.1016/j.apsusc.2021.150682>.

[101] Wang C, Han Y, Li S, Chen T, Yu J, Lu Z. Thermal lithiated-TiO₂: a robust and electron-conducting protection layer for li–si alloy anode. *ACS Appl Mater Interfaces* 2018;10:12750–8. <https://doi.org/10.1021/acsami.8b02150>.

[102] Kim D, Park M, Kim S-M, Shim HC, Hyun S, Han SM. Conversion reaction of nanoporous ZnO for stable electrochemical cycling of binderless si microparticle composite anode. *ACS Nano* 2018;12:10903–13. <https://doi.org/10.1021/acs.nano.8b03951>.

[103] Zhu B, Liu N, McDowell M, Jin Y, Cui Y, Zhu J. Interfacial stabilizing effect of ZnO on si anodes for lithium ion battery. *Nano Energy* 2015;13:620–5. <https://doi.org/10.1016/j.nanoen.2015.03.019>.

[104] Zhou Z-W, Liu Y-T, Xie X-M, Ye X-Y. Constructing novel si@SnO₂ core-shell heterostructures by facile self-assembly of SnO₂ nanowires on silicon hollow nanospheres for large, reversible lithium storage. *ACS Appl Mater Interfaces* 2016;8:7092–100. <https://doi.org/10.1021/acsami.6b00107>.

[105] Si W, Sun X, Liu X, Xi L, Jia Y, Yan C, et al. High areal capacity, micrometer-scale amorphous si film anode based on nanostructured cu foil for li-ion batteries. *J Power Sources* 2014;267:629–34. <https://doi.org/10.1016/j.jpowsour.2014.05.136>.

[106] Grinbom G, Duveau D, Gershinsky G, Monconduit L, Zitoun D. Silicon/hollow γ -Fe₂O₃ nanoparticles as efficient anodes for li-ion batteries. *Chem Mater* 2015;27:2703–10. <https://doi.org/10.1021/acs.chemmater.5b00730>.

[107] Wang G, Zhang J, Zhang Q, Tan X, Li Q, Xie K. In-situ preparation of Nb₂O₅ coated si nanoparticles with pseudocapacitive effect for high-rate lithium ion batteries. *J Electroanal Chem* 2022;904:115945. <https://doi.org/10.1016/j.jelechem.2021.115945>.

[108] Hwa Y, Kim W-S, Yu B-C, Hong S-H, Sohn H-J. Enhancement of the cyclability of a si anode through Co₃O₄ coating by the sol–gel method. *J Phys Chem C* 2013;117:7013–7. <https://doi.org/10.1021/jp401333v>.

[109] Yue L, Tang J, Li F, Xu N, Zhang F, Zhang Q, et al. Enhanced reversible lithium storage in ultrathin

- W18O49 nanowires entwined si composite anode. *Mater Lett* 2017;187:118–22. <https://doi.org/10.1016/j.matlet.2016.10.093>.
- [110] Martinez-Garcia A, Thapa AK, Dharmadasa R, Nguyen TQ, Jasinski J, Druffel TL, et al. High rate and durable, binder free anode based on silicon loaded MoO₃ nanoplatelets. *Sci Rep* 2015;5:10530. <https://doi.org/10.1038/srep10530>.
- [111] Ye J, Chen Z, Hao Q, Xu C, Hou J. One-step mild fabrication of porous core-shelled si@TiO₂ nanocomposite as high performance anode for li-ion batteries. *J Colloid Interface Sci* 2019;536:171–9. <https://doi.org/10.1016/j.jcis.2018.10.029>.
- [112] Zhu J, Wang H, Lin R. Improving the electrochemical performance of silicon materials by SnO₂ through structural design and conductivity. *Appl Surf Sci* 2022;581:152230. <https://doi.org/10.1016/j.apsusc.2021.152230>.
- [113] Hou L, Xiong S, Cui R, Jiang Y, Chen R, Liang W, et al. Three-dimensional porous carbon framework confined si@TiO₂ nanoparticles as anode material for high-capacity lithium-ion batteries. *ChemElectroChem* 2022;9:e202101447. <https://doi.org/10.1002/celec.202101447>.
- [114] Chen Y, Yan Y, Liu X, Zhao Y, Wu X, Zhou J, et al. Porous si/Fe₂O₃ dual network anode for lithium-ion battery application. *Nanomaterials* 2020;10:2331. <https://doi.org/10.3390/nano10122331>.
- [115] Li N, Yi Z, Lin N, Qian Y. An Al₂O₃ coating layer on mesoporous si nanospheres for stable solid electrolyte interphase and high-rate capacity for lithium ion batteries. *Nanoscale* 2019;11:16781–7. <https://doi.org/10.1039/C9NR05264J>.
- [116] Song H, Wang HX, Lin Z, Yu L, Jiang X, Yu Z, et al. Hierarchical nano-branched c-si/SnO₂ nanowires for high areal capacity and stable lithium-ion battery. *Nano Energy* 2016;19:511–21. <https://doi.org/10.1016/j.nanoen.2015.10.031>.
- [117] Yang Y, Yang H-R, Seo H, Kim K, Kim J-H. Novel synthesis of porous si-TiO₂ composite as a high-capacity anode material for li secondary batteries. *J Alloys Compd* 2021;872:159640. <https://doi.org/10.1016/j.jallcom.2021.159640>.
- [118] Jin Y. Self-healing SEI enables full-cell cycling of a silicon-majority anode with a coulombic efficiency exceeding 99.9%. *Energy Env Sci* 2017.
- [119] Yang J, Wang Y, Li W, Wang L, Fan Y, Jiang W, et al. Amorphous TiO₂ shells: a vital elastic buffering layer on silicon nanoparticles for high-performance and safe lithium storage. *Adv Mater* 2017;29:1700523. <https://doi.org/10.1002/adma.201700523>.
- [120] Shi J, Zu L, Gao H, Hu G, Zhang Q. Silicon-based self-assemblies for high volumetric capacity li-ion batteries via effective stress management. *Adv Funct Mater* 2020;30:2002980. <https://doi.org/10.1002/adfm.202002980>.
- [121] Nguyen VA, Kuss C. Review—conducting polymer-based binders for lithium-ion batteries and beyond. *J Electrochem Soc* 2020;167:065501. <https://doi.org/10.1149/1945-7111/ab856b>.
- [122] Ramdhiny MN, Jeon J. Design of multifunctional polymeric binders in silicon anodes for lithium-ion batteries. *Carbon Energy* 2024;6:e356. <https://doi.org/10.1002/cey2.356>.
- [123] Preman AN, Lee H, Yoo J, Kim IT, Saito T, Ahn S. Progress of 3D network binders in silicon anodes for lithium ion batteries. *J Mater Chem A* 2020;8:25548–70. <https://doi.org/10.1039/D0TA07713E>.
- [124] Chen C-H, Wang J-M, Chen W-Y. Conductive polyaniline doped with dodecyl benzene sulfonic acid: Synthesis, characterization, and antistatic application. *Polymers* 2020;12:2970. <https://doi.org/10.3390/polym12122970>.
- [125] Zhang C, Chen Q, Ai X, Li X, Xie Q, Cheng Y, et al. Conductive polyaniline doped with phytic acid as a binder and conductive additive for a commercial silicon anode with enhanced lithium storage properties. *J Mater Chem A* 2020;8:16323–31. <https://doi.org/10.1039/D0TA04389C>.
- [126] Wu C-Y, Kuo P-H, Duh J-G. Reviving of silicon waste with N-doped carbon core-shell structure prepared by vapor deposition polymerization of polypyrrole applied in lithium-ion battery. *Surf Coat Technol* 2021;421:127418. <https://doi.org/10.1016/j.surfcoat.2021.127418>.
- [127] Ryu J, Park S, Hong D, Shin S. Intertwining porous silicon with conducting polymer for high-efficiency stable li-ion battery anodes. *Korean J Chem Eng* 2023;40:497–503. <https://doi.org/10.1007/s11814-022-1227-8>.
- [128] He X, Han R, Jiang P, Chen Y, Liu W. Molecularly engineered conductive polymer binder enables stable lithium storage of si. *Ind Eng Chem Res* 2020;59:2680–8. <https://doi.org/10.1021/acs.iecr.9b05838>.
- [129] Xu Z. Stress-dissipated conductive polymer binders for high-stability silicon anode in lithium-ion batteries 2023.
- [130] Zhao H, Wei Y, Qiao R, Zhu C, Zheng Z, Ling M, et al. Conductive polymer binder for high-tap-density nanosilicon material for lithium-ion battery negative electrode application 2017.
- [131] Zhang S, Chen S, Wang Y, Zhang T, Yue H, Li T, et al. Fabrication of polypyrrole-coated silicon nanoparticle composite electrode for lithium-ion battery. *Ionics* 2024;30:7869–79. <https://doi.org/10.1007/s00033-024-02000-0>.

org/10.1007/s11581-024-05867-w.

[132] Li S, Huang J, Wang J, Han K. Micro-sized porous silicon@PEDOT with high rate capacity and stability for li-ion battery anode. *Mater Lett* 2021;293:129712. <https://doi.org/10.1016/j.matlet.2021.129712>.

[133] Yuca N, Kalafat I, Taskin OS, Arici E. Miscellaneous PEDOT : PTS (polythiophenesulfonyl chloride) based conductive binder for silicon anodes in lithium ion batteries. *Polym Adv Technol* 2023;34:279–86. <https://doi.org/10.1002/pat.5886>.

[134] Higgins TM, Park S-H, King PJ, Zhang C (John), McEvoy N, Berner NC, et al. A commercial conducting polymer as both binder and conductive additive for silicon nanoparticle-based lithium-ion battery negative electrodes. *ACS Nano* 2016;10:3702–13. <https://doi.org/10.1021/acs.nano.6b00218>.

[135] Sandu G, Ernould B, Rolland J, Cheminet N, Brassinne J, Das PR, et al. Mechanochemical synthesis of PEDOT:PSS hydrogels for aqueous formulation of li-ion battery electrodes. *ACS Appl Mater Interfaces* 2017;9:34865–74. <https://doi.org/10.1021/acsami.7b08937>.

[136] Li Z, Liang Z, Ma Z, Qu P, Zhang Y. Boosting the anode performance of the porous si coated with polydopamine and cross-linked with sodium alginate. *J Alloys Compd* 2024;971:172738. <https://doi.org/10.1016/j.jallcom.2023.172738>.

[137] Zhang Y, Wang X, Ma L, Tang R, Zheng X, Zhao F, et al. Polydopamine blended with polyacrylic acid for silicon anode binder with high electrochemical performance. *Powder Technol* 2021;388:393–400. <https://doi.org/10.1016/j.powtec.2021.05.001>.

[138] Zheng H, Fang S, Tong Z, Dou H, Zhang X. Porous silicon@polythiophene core-shell nanospheres for lithium-ion batteries. *Part Part Syst Charact* 2016;33:75–81. <https://doi.org/10.1002/ppsc.201500183>.

[139] Zhou J, Zhou L, Yang L, Chen T, Li J, Pan H, et al. Carbon free silicon/polyaniline hybrid anodes with 3D conductive structures for superior lithium-ion batteries. *Chem Commun* 2020;56:2328–31. <https://doi.org/10.1039/C9CC09132G>.

[140] Pan S, Han J, Wang Y, Li Z, Chen F, Guo Y, et al. Integrating SEI into layered conductive polymer coatings for ultrastable silicon anodes. *Adv Mater* 2022;34:2203617. <https://doi.org/10.1002/adma.202203617>.

[141] Eldona C, Hanif Hawari N, Haidar Hamid F, Dempwolf W, Iskandar F, Peiner E, et al. A free-standing polyaniline/silicon nanowire forest as the anode for lithium-ion batteries. *Chem – Asian J* 2022;17:e202200946. <https://doi.org/10.1002/asia.202200946>.

[142] Lv Y, Shang M, Chen X, Nezhad PS, Niu J. Largely improved battery performance using a micro-sized silicon skeleton caged by polypyrrole as anode. *ACS Nano* 2019;13:12032–41. <https://doi.org/10.1021/acs.nano.9b06301>.

[143] Xia T, Xu C, Dai P, Li X, Lin R, Tang Y, et al. Interpenetrating gels as conducting/adhering matrices enabling high-performance silicon anodes. *J Mater Chem A* 2021;9:12003–8. <https://doi.org/10.1039/D1TA01733K>.

[144] Xu Z, Zheng E, Xiao Z, Shao H, Liu Y, Wang J. Photo-initiated in situ synthesis of polypyrrole fe-coated porous silicon microspheres for high-performance lithium-ion battery anodes. *Chem Eng J* 2023;459:141543. <https://doi.org/10.1016/j.cej.2023.141543>.

[145] Li R, Chen Y, Ding N, Li Z, Li X. Studies on the preparation and electrochemical performance of PSi@poly(3, 4-ethylenedioxythiophene) composites as anode materials for lithium-ion batteries. *J Mater Sci* 2022;57:4323–33. <https://doi.org/10.1007/s10853-022-06922-5>.

[146] Liu X, Xu Z, Iqbal A, Chen M, Ali N, Low C, et al. Chemical coupled PEDOT:PSS/si electrode: suppressed electrolyte consumption enables long-term stability. *Nano-Micro Lett* 2021;13:54. <https://doi.org/10.1007/s40820-020-00564-5>.

[147] Chen B, Xu D, Chai S, Chang Z, Pan A. Enhanced silicon anodes with robust SEI formation enabled by functional conductive binder. *Adv Funct Mater* 2024;34:2401794. <https://doi.org/10.1002/adfm.202401794>.

[148] Luo X, Wu Q, Zhou L, Liu S, Shen X, Lu L. A graded structure of silicon/carbon composite powder for highly stable lithium ion battery anode. *J Alloys Compd* 2024;989:174386. <https://doi.org/10.1016/j.jallcom.2024.174386>.

[149] Huang C, Xu X, Chen D, Lei P. Enhancing rate performance of si@C anode with pore architecture regulated by foaming agent pre-blended with bead mill homogenized si and graphene. *J Energy Storage* 2025;112:115571. <https://doi.org/10.1016/j.est.2025.115571>.